Radiation tolerance of multilayer coating revealed by IBA

H. Khodja, M. Sall, M. Loyer-Prost, C. Cabet, Alain Billard, I. Monnet

Radiation tolerance of multilayer coating revealed by IBA

H. Khodja[(1)], M. Sall[(1)], M. Loyer-Prost[(2)], C. Cabet[(2)], A. Billard[(3)] and I. Monnet[(4)]

(1) LEEL, NIMBE, CEA, CNRS, Université Paris-Saclay, CEA Saclay 91191 Gif-sur-Yvette, France

(2) DEN-Service de Recherches de Métallurgie Physique, CEA, Université Paris-Saclay, F-91191, Gif-sur-Yvette, France

(3) LRC CEA-UTBM LIS-HP, site de Montbéliard, 90010 Belfort cedex, France

(4) CIMAP, CEA – CNRS – ENSICAEN – UCN, BP 5133, 14070 Caen Cedex 5, France

Abstract

Nanostructuration has opened the way for designing materials with improved properties by taking advantage of multiple interfaces providing enhanced local physical properties. In this frame, nanostructured materials are envisioned for nuclear applications due to severe environmental conditions (radiation, temperature, corrosion…). Here we report a study based on IBA (RBS and NRA) of a nanometric Cr/Ta multilayer coating demonstrating an extremely high radiation tolerance. TEM was also performed to confirm RBS results.

Multilayer coated samples were firstly implanted with helium ions, and NRA analyses revealed that an optimized geometry can accommodate up to 20 at. % of gas without noticeable damage, implanted atoms being probably stored at the Cr/Ta interfaces. Heavy ion irradiation was also performed at room temperature (RT) and 400°C, mimicking nuclear reactor neutron bombardment. Although we detected the growth of mixing layers at the Cr/Ta interfaces upon irradiation, these newly created layers remain much thinner than those produced at a single interface, preserving the initial multilayer arrangement.

Keywords: Ion beam mixing, irradiation, Rutherford backscattering spectrometry, multilayer thin films

* Corresponding author; e-mail: hicham.khodja@cea.fr

Introduction

Increasing the intrinsic security and the performance of next generation nuclear plants is a key issue for the development and public acceptance of nuclear energy. One of the conditions to achieve this goal is the elaboration of advanced materials tolerant to a high irradiation dose and to gas accumulation (He and/or H transmutation products under neutron irradiation) at high temperature [1]. In this context, promising research focuses on materials with multiple interfaces (grain and phase boundaries) acting as defect sinks that contribute to reduce the effects of accumulated radiation damage and as traps for implanted species such as helium [2]. Among them, metallic multilayer systems with different interface structures (bcc/fcc, fcc/fcc and bcc/bcc) have attracted much attention during the last decade [3]. The well-controlled high density of interfaces (i.e. small layer thickness) permits to reduce the diffusion distance of point defects, defect clusters and gases from their original location to the nearest sink, and thus considerably limits the formation of damaging extended defects. However, the studied systems were mainly exposed to moderate damage produced by light ions, with the exception of [4]. Thus the major objective of our study is to evaluate the tolerance of metallic multilayer systems to heavy ion irradiation inducing high damage levels by means of Ion Beam Analysis techniques.

Experimental

The most promising metallic multilayer arrangement have incoherent interfaces (bcc/fcc) that present a high density of misfit dislocations acting as defect sinks for radiation-induced point defects and that limit gas bubble growth for example by trapping He bubbles in platelet-shaped cavities [5-6]. However some systems with coherent interfaces also demonstrated a capability to reduce radiation defect formation and helium bubble growth [7]. In our study, we selected a bcc/bcc interface multilayer system made of high melting temperature elements (Cr and Ta, lattice mismatch 12%), an essential requirement for high temperature conditions in nuclear plants. Moreover,

the Cr-Ta system takes advantage of the inherent radiation tolerance of individual metallic component which partially depends on the crystal structure, bcc crystal structure frequently showing better resistance to radiation than fcc one [8].

Multilayer arrangement

Two Cr-Ta multilayers were deposited by physical vapor deposition on silicon wafer substrates. Overall thicknesses of 390 nm and 400 nm were obtained with 15 nm and 50nm-thick individual layers respectively.

Based on the room temperature irradiation results, and as explained in the dedicated section, we prepared a second set of samples with optimized geometries. These multilayers were deposited on a polished Zircaloy plate.

Sample characteristics are summarized in Table 1.

Irradiations

The samples CrTa15 and CrTa50 were implanted at JANNuS-Orsay facility (CSNSM, France) at room temperature (RT) and normal incidence with 50 keV $^{3}He^{+}$ at $2x10^{16}$ and $2x10^{17}cm^{-2}$ fluences. The simulations (SRIM 2008, KP kick mode) predict a peak implanted ^{3}He concentration of about 20 at. % at highest fluence. Heavy ion irradiations were done at JANNuS-Saclay (CEA Paris-Saclay, France) at room temperature (for CrTa15 and CrTa50) and 400°C (for CrTa30 to CrTa100), at normal incidence with 4.5 MeV W^{+} ions to $9x10^{14}$ and $9x10^{15}$ cm^{-2} fluences (for CrTa15 and CrTa50) and 2.5 MeV W^{+} ions $2x10^{16}$ cm^{-2} fluence (for CrTa30 to CrTa100). Both depth distribution profiles of ions and radiation damage were simulated with Monte Carlo by using the code SRIM 2008 [9] in the full cascade mode by considering average displacement energies of 60 and 90 eV for Cr and Ta [10], respectively. The W^{+} ions cross-over the entire multilayers and are mainly implanted in the silicon or Zircaloy substrates, leading to a well-distributed radiation damage over the entire multilayers (in average 45 and 70 dpa in Cr and Ta layers respectively for $9x10^{15}$ cm^{-2} fluence).

Ion Beam Analysis Techniques

Structural characterization of the as-deposited and ^{3}He-implanted or W-irradiated

samples was mainly performed by Rutherford Backscattering Spectroscopy (RBS) using a 2 MeV $^4He^+$ ion beam at 50° off normal incidence to optimize depth resolution, and an annular detector positioned at 170° in IBM geometry. For samples deposited on Zircaloy substrate, combination of two experimental conditions (2.5 MeV at 65° incidence and 2.8 MeV at 50° incidence) proved more efficient by limiting the impact of the large Zr RBS signal. For ^{3}He depth profile measurements, we used Nuclear Reaction Analysis (NRA) technique in the same geometry than for RBS measurements with an incident 540 keV deuterium beam that reacts with implanted ^{3}He to produce alpha particles and protons. Beam was systematically used in scanning mode covering 200x200 μm^2 areas. Typical deposited charges were 1 µC (RBS) and 5 µC (NRA). RBS and NRA spectra were simulated using the SIMNRA and/or MultiSIMNRA softwares [11, 12].

^{3}He profile uncertainties were evaluated by combining quadratically the statistical dispersion from each layer contribution with cross section, charge efficiency collection and solid angle uncertainties, each of the last three parameters fixed to a conservative estimate of 5%.

For some samples we performed Transmission Electron Microscopy (TEM) observations with a FEI Tecnai G2 200 keV microscope and a FEI Tecnai Osiris 300 keV Scanning (S) TEM. TEM lamella were prepared using the Focused Ion Beam (FIB) technique.

Results and discussion

As-grown samples

Figs. 1, 2 show experimental and simulated RBS spectra of pristine CrTa15 and CrTa50 samples, respectively. For the sake of clarity, only the uppermost layer thicknesses are represented in the case of CrTa15 sample. Except for the first Ta layer in the CrTa50 (substrate side), we found the expected multilayer geometry – alternating of Cr and Ta layers both in the CrTa15 and CrTa50 systems with layer thicknesses around 15 nm and 50 nm, respectively, also confirmed by TEM

observations. Other samples show similar results, confirming adequate layer arrangements and thicknesses.

Room Temperature irradiated samples

Helium implantation

We compare in Fig. 3a and 3b the He depth profiles measured by NRA in CrTa15 and in CrTa50 implanted at fluences of $2x10^{16}$ cm^{-2} and $2x10^{17}$ cm^{-2}. For CrTa15, the ^3He profiles at the two fluences are Gaussian-shaped and very similar, suggesting that He retention efficiency is comparable for the two implantation doses in CrTa15. On the contrary, profiles in CrTa50 are asymmetric and different for the two fluences, with up to 4 at. % ^3He at the surface for the $2x10^{17}$ cm^{-2} fluence, revealing that the trapping of ^3He in Cr-Ta multilayers is improved as the interface density increases. Though TEM observations are needed to determine whether ^3He atoms are mainly trapped at interfaces or reside preferentially in one or the other of the Cr or Ta layers, the absence of ^3He diffusion in the CrTa15 sample after implantation at 20 at. % demonstrates comparable retention performances of Cr-Ta system and Cu-Nb state-of-art system [13].

Heavy ion irradiation

The main concern of radiation effect in multilayer systems is probably the formation of mixing layers that may alter the multilayer structure and thus the interface sinks for point defects and gases. After irradiation with 4.5 MeV W^+ ions at the highest fluence, the best fit with MultiSIMNRA of the CrTa50 RBS spectrum was obtained by introducing mixing layers between the native Cr and Ta layers (Fig. 4a). We assumed for the mixing layers a stoichiometry of $CrTa_2$ which is consistent with TEM observations (Fig. 4b) as the RBS measured mixing layer thickness (assuming nominal atomic density) is close to the TEM ones. However it clearly appears from a STEM EDS map (not shown) that the mixing layer does not have a fixed stoichiometry, but rather that a gradient of concentration from one element to the other exists. $CrTa_2$ is thus an average stoichiometry over the entire thickness of the mixing layer. Excellent consistency is obtained between the experimental spectrum

and the best fit with a mixing layer thickness of about 10 nm (Fig. 4a).

While mixing layer thicknesses in CrTa15 and CrTa50 both irradiated at $9x10^{14}$ cm^{-2} were successfully determined by RBS measurements, the mixing layers thicknesses in CrTa15 system W-irradiated at $9x10^{15}$ cm^{-2} were estimated from TEM observations. Although the multilayer pattern is preserved (Fig. 5b), it presents a wavy structure explaining the loss of the RBS oscillatory shape (Fig. 5a). The waviness probably initiates from the interface with the silicon substrate which has been highly irradiated by the implanted W^+ ions.

High temperature-irradiated samples

As observed in Fig. 4a, Ta is more likely to be consumed during irradiation by the mixing layer growth process, thus the second set of samples was adjusted by increasing the Ta to Cr ratio (Table 1). These irradiations were performed using a higher fluence (W^+ 2.5 MeV $2x10^{16}$ cm^{-2}) inducing damage ranging from ~40 dpa (first Cr layer, substrate side) to ~200 dpa (last Ta layer, vacuum side).

While above ~100 dpa a complete mixing has occurred, we noticed that samples were partially preserved, as illustrated for CrTa30 in Fig 6. One should note again the good agreement between (indirect) IBA and (visual) TEM mixing layer thickness evaluations.

Comparison with thermal spike model

Several phenomenological models have been developed to explain ion beam mixing at metal interfaces such as the ballistic mixing model [14] and the thermal spike (TS) model [15]. The ballistic model assumes ion beam mixing is only dependent on the kinematics of the ion-material interaction. However, in many bilayer systems, the measured mixing rate highly differs from the value calculated by the ballistic model. This has been attributed to the influence of chemical potential gradients across the interface, particularly when high energy primary knock-on atoms (PKA) are produced [16]. Regardless of the structure (coherent or incoherent), interfaces with atomic elements of positive heat of mixing present an inherent better resistance to radiation as chemical driving forces can avoid radiation induced atomic intermixing. The TS

model is based on a thermodynamic concept where the relaxation (thermalizing) subsequent to atomic collision cascades results in an increase of the local temperature up to 10^3 – 10^4 K (thermal spike), generally higher than the melting temperature of the individual elements. The atomic interdiffusion at the interface prior to the rapid quenching of the molten zone depends on both the heat of mixing and the cohesive energy of the two elements. The TS model is temperature independent and has accurately predicted mixing rates in various irradiated bilayer systems [15]. The mixing rate according to this model is:

$$k = \frac{d(2\tilde{D}t)}{d\phi} = \frac{1}{2}\frac{K_1 F_D^2}{\bar{N}^{5/3}(\Delta H_{coh})^2}\left(1 + K_2\frac{\Delta H_{mix}}{\Delta H_{coh}}\right)$$

where $\sigma^2 = 2\tilde{D}t$ is the variance of the interdiffusion profile (i.e. square of the mixing layer thickness) and Φ the ion fluence. K_1 = 0.0035 nm and K_2= 27.4 are phenomenological parameters, while for Cr-Ta interfaces ΔH_{coh} = 5.51 eV/atom [16] and ΔH_{mix} = - 0.093 eV/atom [17]. $\bar{N}$ = 6.93 x 10^{22} at.cm^{-3} is the average atomic density of the two elements and F_D is the energy deposited at the interface by nuclear collisions. At the uppermost Cr-Ta multilayer interfaces, SRIM calculation gives F_D = 4.9 keV/nm with 4.5 MeV W^+ ion. The calculated mixing rate k ranges from 2.51 to 4.59 nm^4.

Fig. 7 presents the comparison of experimental mixing layer thicknesses with predicted ones. Experimental thicknesses are smaller than those calculated by the TS model. This favorable discrepancy may be attributed to the availability of nearby interfaces acting as defect sinks. We can notice that at RT CrTa15 exhibits a mixing layer 3 times thinner than the one calculated by the TS model. At higher temperature and higher damage, we also point out the good performance of the CrTa30 layer arrangement, at least up to ~100 dpa.

Conclusion and prospects

We have demonstrated using Ion Beam Analysis techniques that Cr-Ta multilayers

show high tolerance to either heavy ion irradiation or ^{3}He implantation. These systems may contain ^{3}He at concentrations up to 20 at. % without a noticeable post-implantation diffusion for high interface density multilayers. Though layer mixing is promoted under heavy ion irradiation for Cr-Ta multilayers by the negative heat of mixing of the elements, the nanometric multilayer character remains for radiation damage up to ~100 dpa. Furthermore, the mixing layer thickness decreases as the period-thickness of the multilayers decreases, confirming the important role of the interface density on irradiation defect recovery, as also observed in [4]. The comparison to the thermal spike model, well-tuned for bilayer systems, suggests a significant recovery during damage production at RT and 400°C as well.

Additional studies including ^{3}He implantations on pre-irradiated samples should further assess the advantages of Cr-Ta multilayers use in nuclear environment.

Acknowledgments

This work was granted by the CEA Cross-Cutting programs “Advanced Materials” and “Nanosciences”.

References

[1] P. Yvon, M. Le Flem, C. Cabet, J.L. Seran, Structural materials for next generation nuclear systems: Challenges and the path forward, Nucl. Eng.Des. 294 (2015) 161-169.

[2] G. Ackland, Controlling Radiation Damage, Science, 327 (2010) 1587-1588.

[3] I.J. Beyerlein, M.J. Demkowicz, A. Misra, B.P. Uberuaga, Defect-interface interactions, Prog. Mat. Sc. 74 (2015) 125-210.

[4] L. Dong, H. Zhang , H. Amekura , F. Ren, A. Chettah, M. Hong, W. Qin, J. Tang, L. Hu, H. Wang, C. Jiang, Period-thickness dependent responses of Cu/W multilayered nanofilms to ions irradiation under different ion energies, J. Nucl. Mater. 497 (2017) 117-127.

[5] M.J. Demkowicz, D. Bhattacharyya, I. Usov, Y.Q. Wang, M. Nastasi, A. Misra,

The effect of excess atomic volume on He bubble formation at fcc–bcc interfaces, App. Phys. Lett. 97 (2010) 161903.

[6] S. Mao, S. Shu, J. Zhou, R.S. Averback, S.J. Dillon, Quantitative comparison of sink efficiency of Cu-Nb, Cu–V and Cu–Ni interfaces for point defects, Acta Mater. 82 (2015) 328-335.

[7] Y. Chen, Y. Liu, E.G. Fu, C. Sun, K.Y. Yu, M. Song, J. Li, Y.Q. Wang, H. Wang, X. Zhang, Unusual size-dependent strengthening mechanisms in helium ion-irradiated immiscible coherent Cu/Co nanolayers, Acta Mater. 84 (2015) 393-404.

[8] M. Victoria, N. Baluc, C. Bailat, Y. Dai, M.I. Luppo, R. Schäublin, B.N. Singh, The microstructure and associated tensile properties of irradiated fcc and bcc metals, J. Nucl. Mater. 276 (2000) 114-122.

[9] J.F. Ziegler, J.P. Biersack, M.D. Ziegler, SRIM - The Stopping and Range of Ions in Matter, SRIM Company, 2008.

[10] M. Nastasi, J. Mayer, J.K. Hirvonen, Ion-Solid Interactions: Fundamentals and Applications, Cambridge University Press, 1996.

[11] M. Mayer, SIMNRA, a simulation program for the analysis of NRA, RBS and ERDA, AIP Conference Proceedings, 475 (1999) 541-544.

[12] T.F. Silva, C.L. Rodrigues, M. Mayer, M.V. Moro, G.F. Trindade, F.R. Aguirre, N. Added, M.A. Rizzutto, M.H. Tabacniks, MultiSIMNRA: A computational tool for self-consistent ion beam analysis using SIMNRA, Nucl. Instrum. Meth. B 371 (2016) 86-89.

[13] M.J. Demkowicz, Y.Q. Wang, R.G. Hoagland, O. Anderoglu, Mechanisms of He escape during implantation in CuNb multilayer composites, Nucl. Instrum. Meth. B 261 (2007) 524-528.

[14] P. Sigmund, A. Gras-Marti, Theoretical aspects of atomic mixing by ion beams, Nucl. Instrum. Meth. 182 (1981) 25-41.

[15] W.L. Johnson, Y.T. Cheng, M. Van Rossum, M.A. Nicolet, When is thermodynamics relevant to ion-induced atomic rearrangements in metals? Nucl. Instrum. Meth. B 7 (1985) 657-665.

[16] C. Kittel, Introduction to Solid State Physics, Wiley, 2004.

[17] M. Venkatraman, J.P. Neumann, The Cr−Ta (Chromium-Tantalum) system, JPE, 8 (1987) 112-116.

Table 1

Sample	e_{Cr} (nm)	e_{Ta} (nm)	N layers	Substrate
CrTa15	15	15	13 + 13	Si
CrTa50	50	50	4 + 4	Si
CrTa30	24	36	3 + 3	Zr
CrTa100	80	120	1 + 1	Zr

Table 1: Sample multilayer arrangement. e_{Cr}, e_{Ta}: Cr and Ta layer thicknesses; N layers: Cr layers + Ta layers

Figure 1

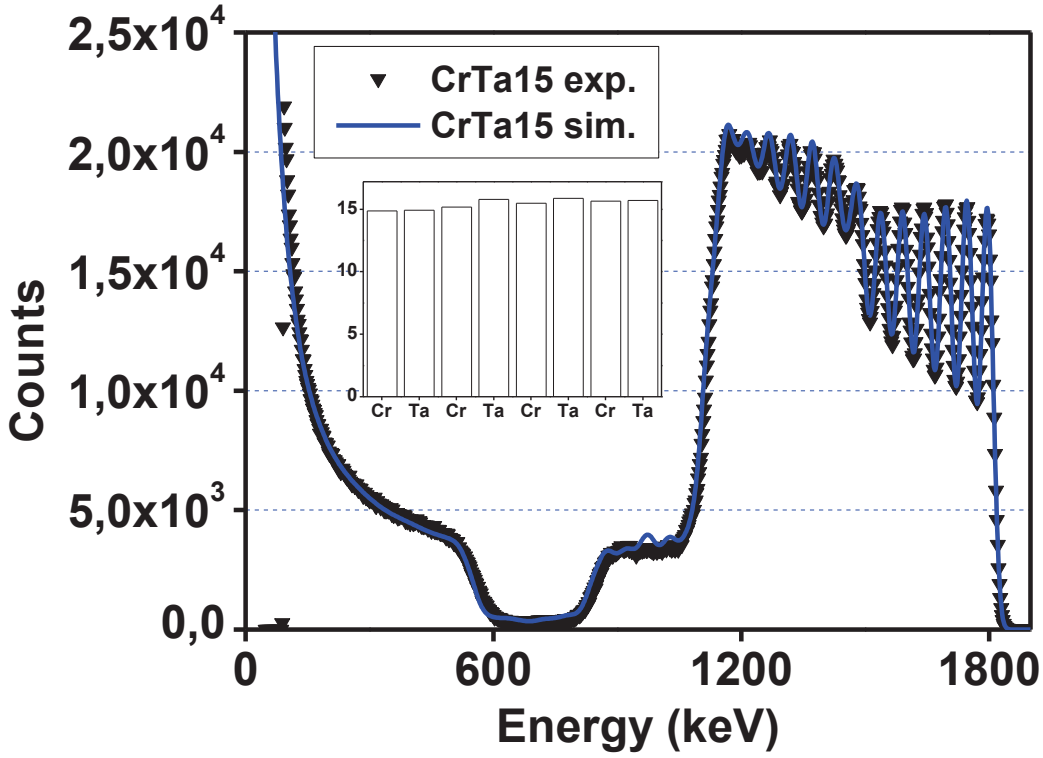
2,5x10^4
2,0x10^4
1,5x10^4
1,0x10^4
5,0x10^3
0,0
Counts
0
600
1200
1800
Energy (keV)
CrTa15 exp.
CrTa15 sim.
15
10
5
0
Cr Ta Cr Ta Cr Ta Cr Ta

Figure 2

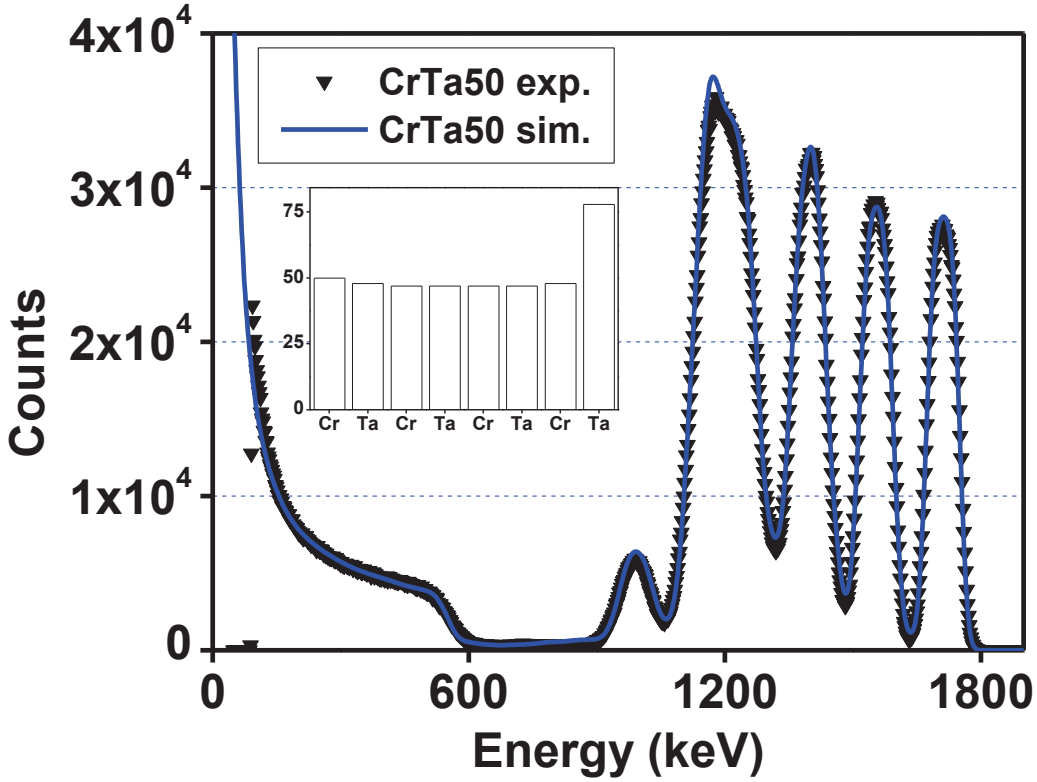
4x10^4
3x10^4
2x10^4
1x10^4
0
Counts
0
600
1200
1800
Energy (keV)
CrTa50 exp.
CrTa50 sim.
75
50
25
0
Cr Ta Cr Ta Cr Ta Cr Ta

Figure 3

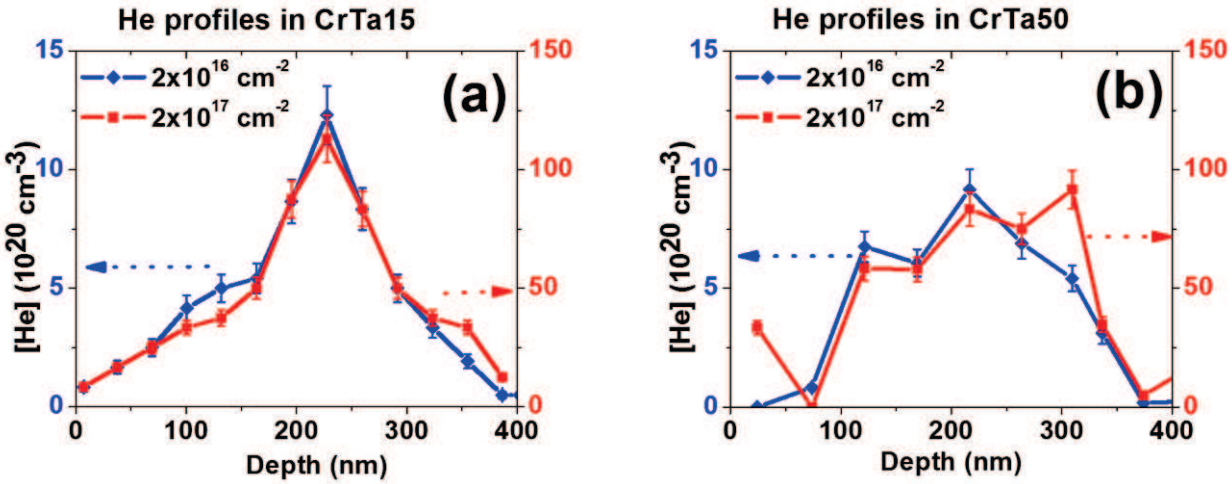
He profiles in CrTa15
2x10^16 cm^-2
2x10^17 cm^-2
(a)
[He] (10^20 cm^-3)
Depth (nm)
He profiles in CrTa50
2x10^16 cm^-2
2x10^17 cm^-2
(b)
[He] (10^20 cm^-3)
Depth (nm)

Figure 4

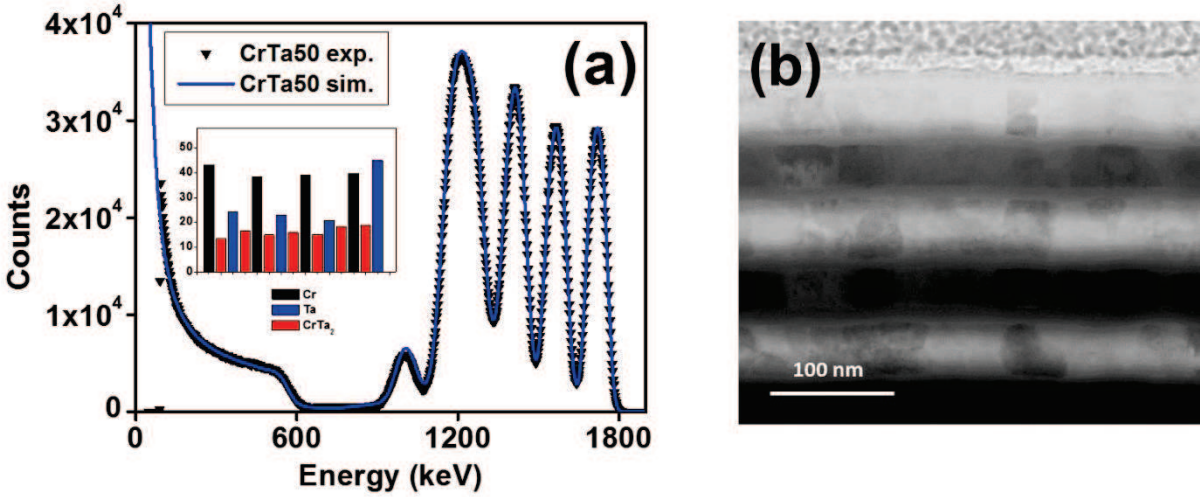

Figure 5

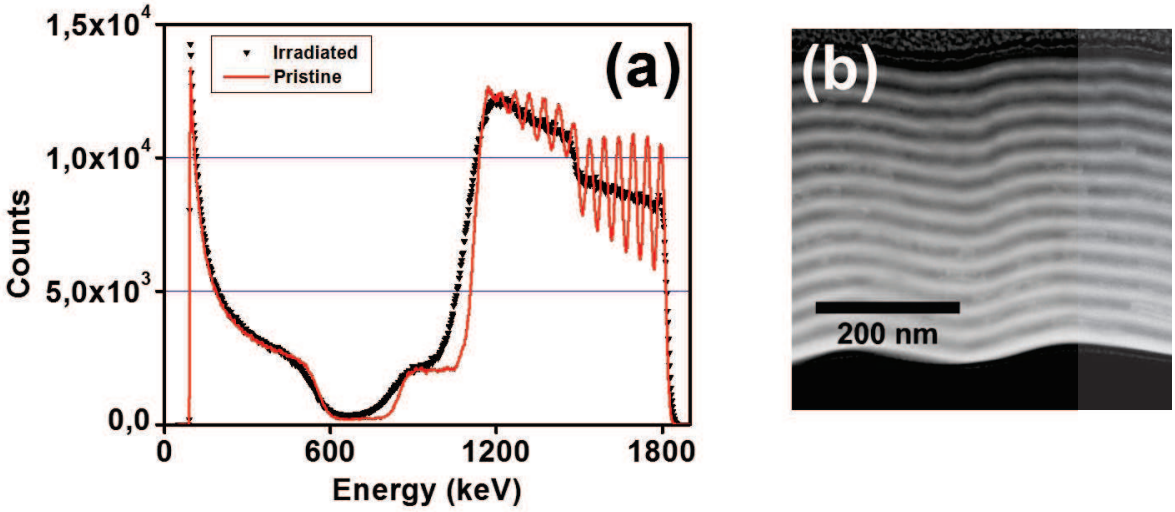
(a)
Irradiated
Pristine
Counts
1,5x10^4
1,0x10^4
5,0x10^3
0,0
0
600
1200
1800
Energy (keV)
(b)
200 nm

Figure 6

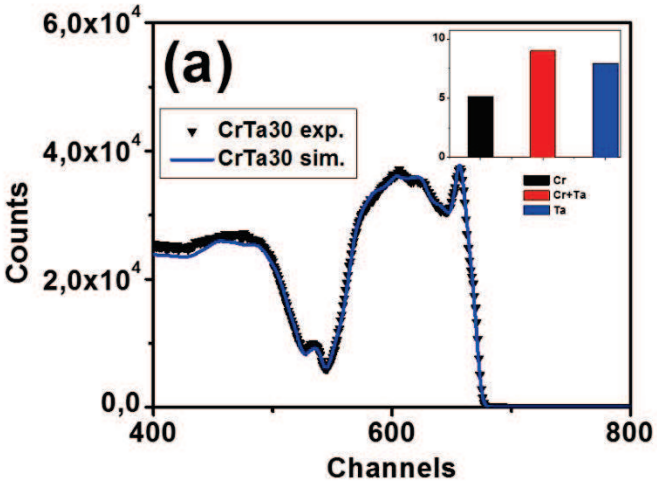
(a)
CrTa30 exp.
CrTa30 sim.
Cr
Cr+Ta
Ta
Counts
Channels
6,0x10^4
4,0x10^4
2,0x10^4
0,0
400
600
800

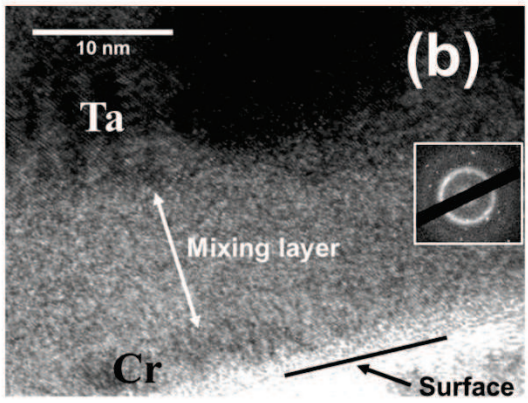
10 nm
(b)
Ta
Mixing layer
Cr
Surface

Figure 7

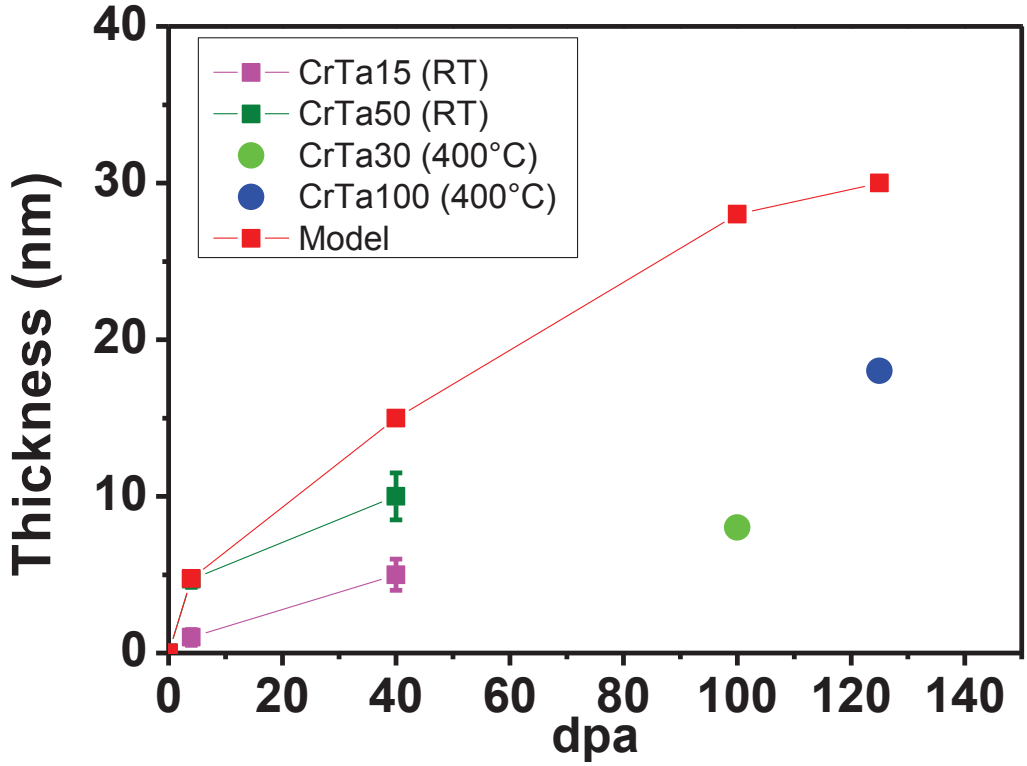
CrTa15 (RT)
CrTa50 (RT)
CrTa30 (400°C)
CrTa100 (400°C)
Model
Thickness (nm)
dpa
0
10
20
30
40
0
20
40
60
80
100
120
140

Figure 1: RBS spectrum and inset: layer thicknesses (in nm) from pristine CrTa15

Figure 2: RBS spectrum and inset: layer thicknesses (in nm) from pristine CrTa50

Figure 3: ^{3}He profiles from NRA at two implantation fluences: 2e16 at.cm-2 (blue) and 2e17 at.cm-2 (red) in (a) CrTa15 and (b) CrTa50

Figure 4: RBS spectrum and inset: layer thicknesses (in nm) from irradiated CrTa50 (a) and corresponding TEM image (b)

Figure 5: RBS spectrum from irradiated CrTa15 (a) and corresponding TEM image (b)

Figure 6: RBS spectrum and inset: layer thicknesses (in nm) from irradiated CrTa30 (a) and corresponding TEM image (b)

Figure 7: Experimental mixing layer data and TS model predictions